Rationalization of the Synthesis of SBA-16: Controlling the Micro- and Mesoporosity

Pascal Van Der Voort,* Mina Benjelloun, and Etienne F. Vansant

University of Antwerp (U.I.A.), Department of Chemistry, Laboratory of Adsorption and Catalysis, Universiteitsplein 1, B-2610 Wilrijk, Belgium

Received: May 15, 2002; In Final Form: June 26, 2002

The effects of the synthesis parameters on the properties of the cubic *Im*3*m* SBA-16 have been investigated systematically for the first time. We show that the total pore volume, pore diameter, and ratio micro-/mesopores can be controlled very efficiently by changing the synthesis time, temperature, and the TEOS/surfactant ratio. We also argue that at high TEOS/surfactant ratios, structures with internal microporous nanocapsules will be created. These materials have unprecedentedly high micropore contributions, which can comprise up to 65% of the total pore volume.

Introduction

The family of Mesoporous Templated Structures (MTS) is expanding continuously. Following the earlier reports on M41S materials,[1,2] many new types of materials were developed, such as FSM-16,[3] various MSU materials,[4] KIT,[5] and many SBA materials.[6,7]

To be applicable as a superior catalyst support or adsorbent, these materials should meet a number of minimal requirements, such as a good stability in working conditions, a fairly inexpensive, simple, and ecologically friendly synthesis method and unambiguous criteria to evaluate the quality of the final material. Secondary, but also very important, requirements include a good accessibility of the pores for the reagents and a combined and controllable micro- and mesoporosity. The combined micro- and mesoporosity can greatly enhance the activity and selectivity of the catalyst. The accessibility of the pores, especially in thin film configurations, is best achieved by a three-dimensional porous structure.

The SBA-15 and SBA-16 materials meet most of these objectives. They are synthesized by the environmentally friendly triblock copolymers, which can, if desired, be regenerated and reused.[6] They have intrinsically both micro- and mesopores in their structure and possess relatively thick walls (3−4 nm compared to typical values of 1 nm for MCM-41, MCM-48, FSM,...). Their thermal, hydrothermal and mechanical stability is very good, compared to the more often used MCM-41 and MCM-48.

The optimization of the synthesis of the hexagonal SBA-15,[8,9] its catalytic activation,[10,11] its surface modification and subsequent use as selective adsorbent[12−14] has received a lot of attention the past few years. The cubic counterpart, SBA-16, has not been studied very extensively. This is probably due to the difficulties encountered in the synthesis and especially in the characterization of this material. In 2000, Sakamoto et al.[15] were finally able to present a clear model for the structure of SBA-16, based on high-resolution TEM.

A general problem of cubic systems is the difficulty in assessing the wall thickness in a simple way. Fortunately, following a procedure to estimate the wall thickness of MCM-48,[16] Ravikovitch and Neimark[17] have recently published a very simple way to calculate the wall thickness of the cubic *Im*3*m* structure of SBA-16.

There is no doubt that SBA-16 is a very important MTS material. Therefore, we present here for the first time a systematic study of the factors that influence the properties (wall thickness, pore size, and relative and absolute amounts of micro- and mesopores) of the SBA-16 cubic material.

Experimental Section

Synthesis of Materials. SBA-16 is synthesized using Pluronic F127 ($EO_{106}PO_{70}EO_{106}$) as the structure-directing agent and TEOS as the silica source. In a typical synthesis, 4 g of F127 was dissolved in 30 g of deionized water and 120 g of HCl (2M) at 25−65 °C. A chosen amount of TEOS (between 5 and 15 g) is added to the solution. The mixture is maintained at 25−65 °C for different times from 4 h to 20 h with vigorous stirring, followed by heating at 65−100 °C for different times from 15 h to 48 h.

The solid products were filtered off and then washed with deionized water repeatedly. After drying at room-temperature overnight, the products were calcined in ambient air from room temperature up to 550 °C with a heating rate of 2 °C/min.

Characterization. X-ray diffraction measurements were performed on a Phillips PW 1840 powder diffractometer, using Ni-filtered with Cu Kα radiation. Nitrogen adsorption−desorption isotherms were recorded on a Quantachrome Autosorb-MP automated gas adsorption system. The calcined samples were degassed at 200 °C for 16 h prior to analysis.

SEM measurements were recorded on a JEOL-JSM-6300 scanning electron microscope, operating at an acceleration voltage of 20−30 kV. Prior to analysis, the samples were sputtered with a thin film of carbon.

Results and Discussion

SBA-16 is a mesoporous templated structure with the cubic *Im*3*m* symmetry. Its best representation is by a triply periodic minimal surface, type I−WP or C(P). Representations of these structures can be found elsewhere.[15]

* To whom correspondence should be addressed. E-mail: pascal.vandervoort@ua.ac.be.

10.1021/jp0261152 CCC: $22.00
Published on Web 08/09/2002

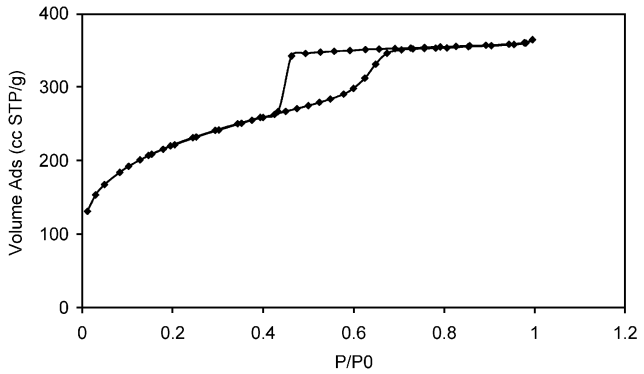

Figure 1. Nitrogen adsorption−desorption isotherm and BJH pore size distribution of a high quality SBA-16.

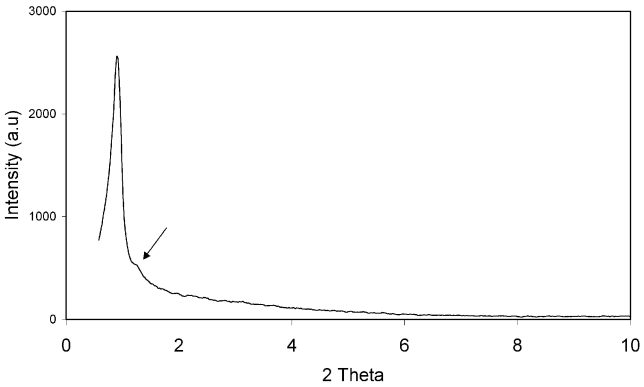

Figure 2. X-ray Diffractogram of a high quality SBA-16.

We have prepared a standard high quality SBA-16 by a modified and fast synthesis procedure, as described above, using a stirring time of 8 h at 40 °C, followed by an aging period of 24 h at 80 °C. The N_2 adsorption−desorption isotherm of this calcined SBA-16 and its pore size distribution are presented in Figure 1. The very typical adsorption−desorption hysteresis (indicative for ink-bottle pores), closing just above $p/p° = 0.45$ has been examined in detail by Ravikovitch et al.[17] and fully complies with the non local density functional theory. The pore size distribution, calculated on the adsorption isotherm, shows a narrow distribution of large mesopores, distributed around an average pore diameter of 5.4 nm. The total surface area as calculated by the BET method is 754 m^2/g. A t-plot analysis reveals an important fraction of micropores. The total pore volume of this material is 0.45 cm^3/g, the micropore volume is 0.22 cm^3/g, which is almost 50%!

The micropores originate from the penetration of the EO chains of the triblock copolymer in the silica walls, thus creating intrawall porosity, connecting the different mesoporous cavities.

The XRD patterns of calcined SBA-16 (Figure 2) shows a very strong 110 reflection (1.01 ° 2θ) of the cubic *Im*3*m* structure and a small shoulder of the 200 reflection (1.42 ° 2θ). Both reflections yield an a_0 value of 12.4 nm, confirming that the measured structure is indeed the *Im*3*m* SBA-16 structure, as the shoulder would be at a completely different position for a hexagonal or lamellar structure.

The pore wall thickness of SBA-16 can be calculated by a simple formula[17]

$$< h > = \frac{\sqrt{3}\cdot a_0}{2} - D_{\mathrm{me}}$$

D_{me} is the mesopore diameter, and a_0 is the unit cell parameter as calculated from the XRD patterns. The wall thickness of the SBA-16, presented in Figures 1 and 2, is calculated using the a_0 value from the X-ray Diffractogram (12.4 nm) to be 5.3 nm. This means that the average wall thickness is around the same magnitude as the pore diameter, both having a value that is slightly above 5 nm. It should be stressed that the walls of SBA-16 are therefore more than 5 times thicker than for its MCM-48 cubic or MCM-41 hexagonal counterparts.

Effects of the Temperature. Until now, no systematic studies have appeared on the effect of the synthesis or aging temperature on the porosity of SBA-16. For the hexagonal SBA-15 material, it has been suggested in the literature that the temperature has a significant impact of the final porosity of the sample because of the temperature-dependent behavior of the $(EO)_x(PO)_y(EO)_x$ triblock copolymers in acidic media.[6,18,19] The PO block of the polymer is strongly hydrophobic, whereas the hydrophobicity of the EO blocks is strongly dependent on the temperature of the synthesis mixture.

As the hydrophobicity of the EO blocks increases as a function of the temperature, the degree of hydration of these EO blocks decreases dramatically at higher temperatures.

This implies a lower interaction with water molecules and a withdrawal of the EO chains inside the hydrophobic core of the surfactant, resulting in a larger volume of the micelle core and therefore a higher pore volume of the SBA-15 material. Also, as a function of increasing temperature, the average pore diameter increases, and the relative amount of micropores decreases.

However, we have performed in this study a more detailed investigation of this effect. As the synthesis of both SBA-15 and SBA-16 consists of gel formation step and an aging step, we have investigated the effect of the temperature in both steps separately. The results suggest that the model described above needs some refinement.

Figure 3A shows the evolution of the porosity of the SBA-16 samples, as a function of the *stirring temperature* (gel formation), whereas all other parameters are held constant. After stirring 8 h at the indicated temperature, the samples were aged for 24 h at 80 °C, filtered, and calcined.

It can be inferred from this figure that the total pore volume *decreases* as a function of the stirring temperature. The relative amount of micro-and mesopores is relatively constant. Figure 3C (dashed line) shows the effect of the stirring temperature on the pore size; it can be inferred from this figure that the stirring temperature has no significant effect on the final pore radius.

Figure 3B on the other hand shows the evolution of the porosity of the SBA-16 samples as a function of the *aging temperature*, whereas all other parameter were held constant (stirring temperature in this case was set at 45 °C). Figure 3B shows that the total pore volume of the samples *increases* as a function of the aging temperature. In this case, there is a very clear relation between the aging temperature and the relative amount of micro- and mesopores: at increasing aging temperatures, the relative (and absolute) amount of micropores strongly decreases. Also, Figure 3C (solid line) shows a very clear relation between the average pore size and the aging temperature: the pore size of the SBA-16 increases as a function of increasing aging temperature.

The different trends in Figures 3A and 3B clearly suggest that two different mechanisms are at work. During the initial stages of the synthesis (stirring of the reagents, hydrolysis, polymerization, and condensation of the TEOS), an increase of the temperature results in a higher hydrophobicity of the EO chains; therefore in a lower hydration of these chains and a

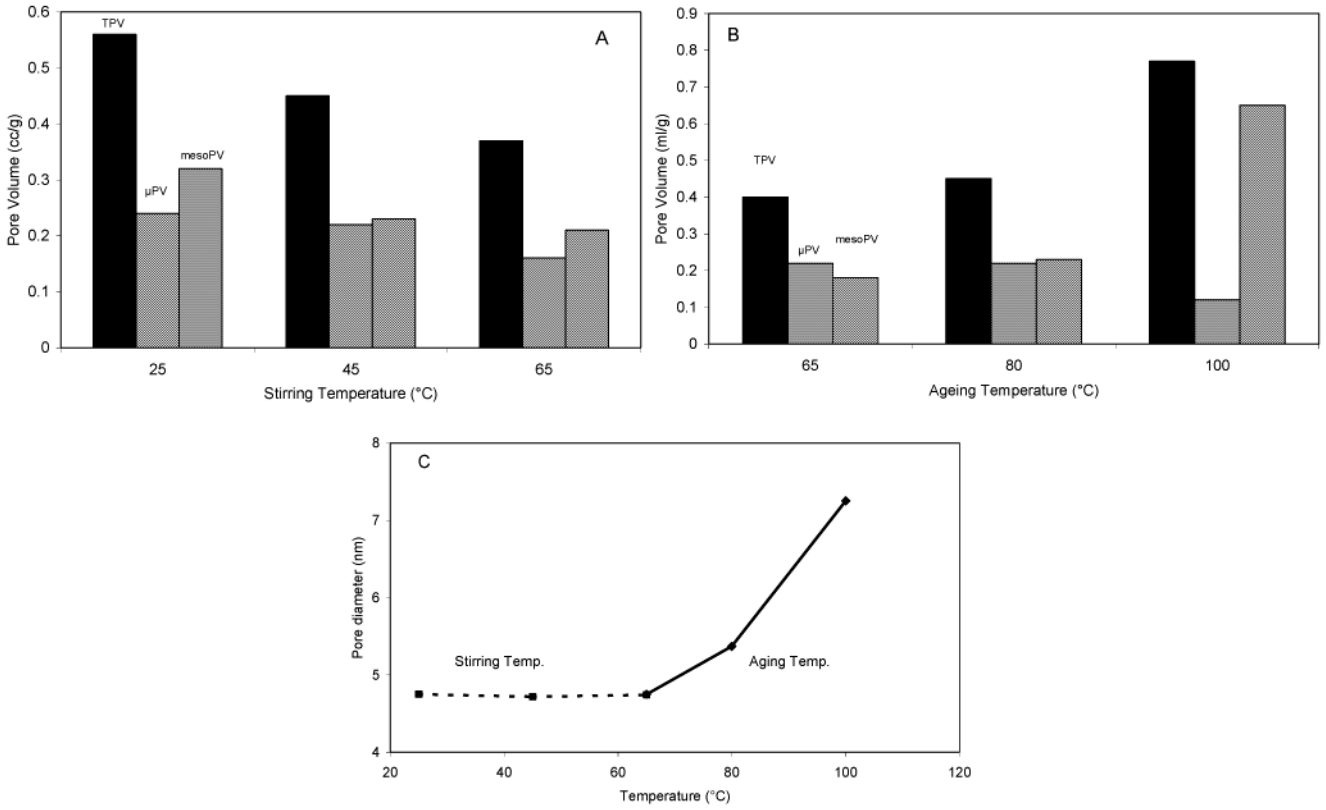

Figure 3. Total pore volume, micro- and mesopore volume as a function of the stirring temperature with constant aging temperature (A) and as a function of the aging temperature with constant stirring temperature (B); evolution of the pore diameter as a function of aging and stirring temperatures (C).

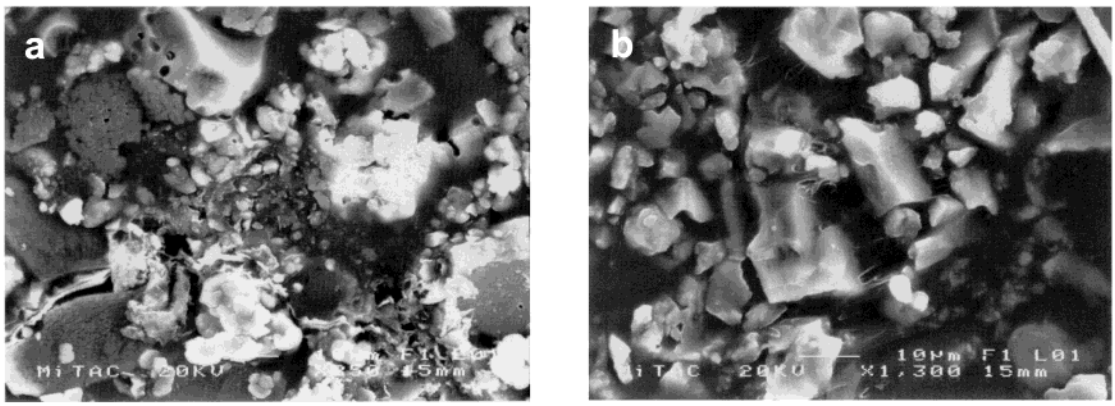

Figure 4. SEM picture of (a) SBA-16, stirring temperature 65 °C, aging temperature 80 °C; (b) SBA-16, stirring temperature 45 °C, aging temperature 80 °C.

weaker and lesser interaction with the positively charged silicate species in solution. The reader is reminded that the interaction between the surfactant and the silica source occurs through a Cl-bridge, between the positively charged surfactant and the positively charged silicate species, as $(EO)-(H_3O)^+$-$Cl^-(Si-O)^+$, as described in the original publication of Stucky's group.[6] The very weak interaction, combined with the increased rate of hydrolysis and polymerization of the TEOS source at higher temperatures, results in the formation of a higher amount of amorphous silica, which has a negligible contribution to the total pore volume. At lower stirring temperatures, the (EO) chains are more hydrophilic and interact stronger and more with the silicate cations, resulting in a more ordered structure and a lower amount of amorphous silica.

This is clearly illustrated in Figure 4. Figure 4, parts (a) and (b), shows the differences in crystallinity of the SBA-15 when the stirring temperature is decreased from 65 °C to 45 °C, whereas the aging temperature is kept constant at 80 °C. Part (b) clearly shows a SBA-16 sample which is highly crystalline, with predominantly cubic crystals. At higher stirring temperatures (picture a), a significant fractions of amorphous silica are present, which is due to the lesser interaction with the surfactant chains.

During the later stages of the synthesis (aging of the gel), a different mechanism occurs. When the aging temperature is increased, the (EO) chains will become more hydrophobic and will withdraw inside the hydrophobic (PO) core, leaving holes or voids in the silica walls. These holes or voids, however, are too unstable to resist the calcination. In other words, after calcination, micropores will only be generated at places when the (EO) is *actively* penetrating the silica wall.

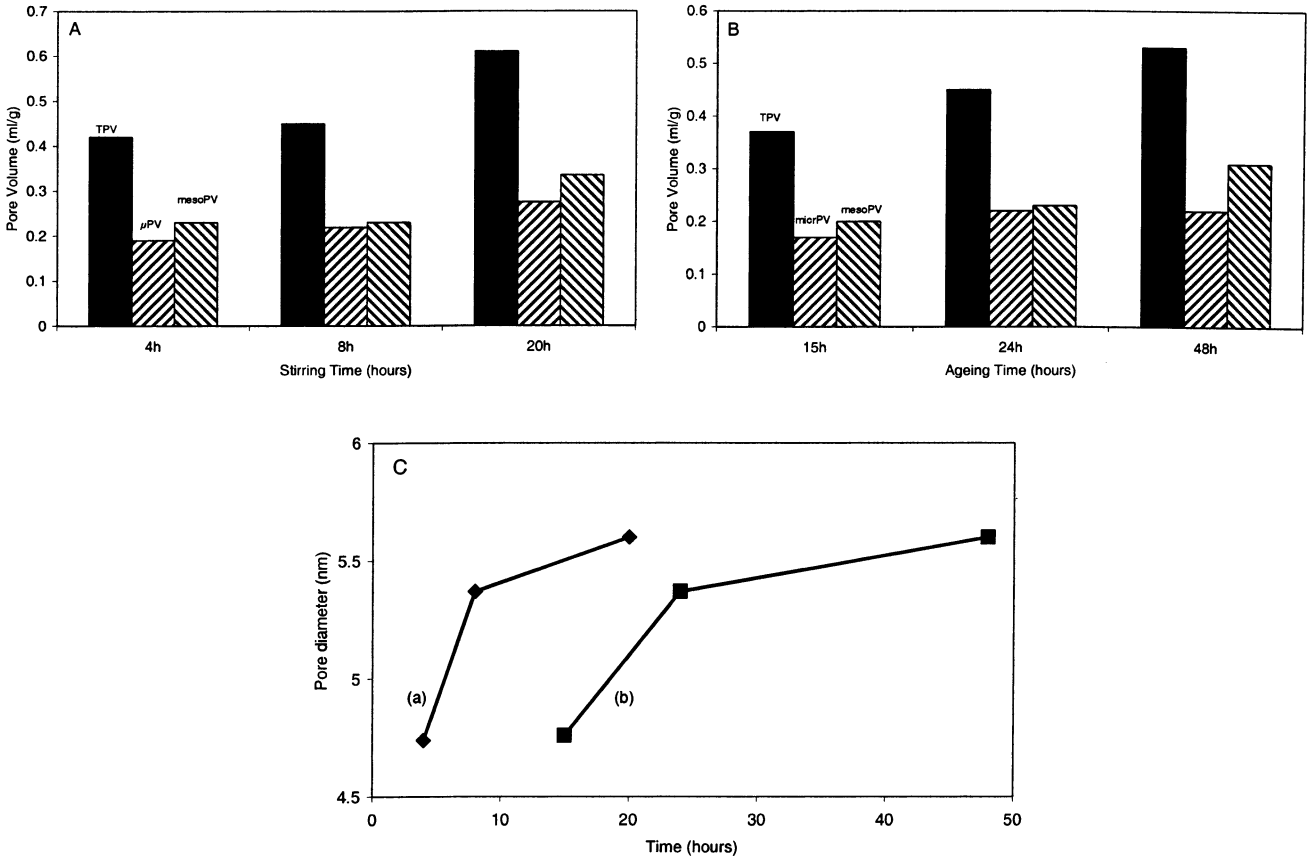

Figure 5. (A,B): Evolution of total, micro- and mesopore volume as a function of (A) stirring time and (B) aging time. (C): Evolution of pore diameter as a function of (a) stirring time and (b) aging time. Each time the other parameters are held constant (stirring temperature = 45 °C, aging temperature: 80 °C, TEOS/surfactant ratio = 60).

A very similar observation was made by Kruk and Jaroniec[18] for the hexagonal SBA-15 counterpart. They observed a strong unit cell shrinkage and a reduction of the microporosity upon calcination if the precursor was washed more intensively. They suggested that the washing procedure not only removes the polymer template which occupies the primary mesopores, but also reduces the amount of (EO) chains in the silica walls, which in turn created void spaces in the walls. The increased shrinkage of the unit cell upon calcination after washing corroborates our suggestion that the empty voids in the silica wall of the precursor are not stable toward calcination (shrinkage of the unit cell) and therefore explains the reduction of the micropores.

Therefore, we can state that the large reduction of micropores as a function on increasing aging temperatures is caused by an increasing withdrawal of the EO chains from the silica walls, leaving voids which are too unstable to produce micropores after calcination.

The increase in the total pore volume and the pore size as a function of the aging temperature complies with this mechanism. Upon increasing temperature, the EO chains will penetrate more and more the hydrophobic PO core, resulting in materials with a higher pore volume and a larger pore size.

Optimization of the porosity of SBA-16 (and by extrapolation SBA-15) will have to take both aspects into account. In the initial stages, a temperature has to be found that on one hand guarantees a good hydrolysis and polymerization of the TEOS source, but on the other hand leaves the EO chains sufficiently hydrated to obtain a good interaction between the surfactant and the silicate cations. In the subsequent stages (aging), a controlled pore size engineering is possible by a good selection of the aging temperature, which highly influences the pore volume, pore size and microporosity of the final sample.

Effects of the Time. The effect of the synthesis time on the properties of the SBA-16 has been investigated, again making a distinction between the stirring time and the aging time. Stirring temperature was kept constant at 45 °C, aging temperature at 80 °C and the TEOS/P127 ratio at 60. Figure 5(A,B,C) show these effects on the porosity of the samples. Figure 5 (A,B) shows that both the stirring time as the aging time affect the total pore volume of the material (pore volume increases with increasing times), but does not affect in a significant way the relative amount of micro- and mesopores. The relative amount of micropores is constant at 40−50% of the total porosity. The pore diameter (Figure 5C) increases strongly at the low synthesis times, after which it more or less reaches a plateau.

These figures indicate that a stirring time of more than 8 h and an aging time of more than 24 h is needed to reach a state of equilibrium. We presume that at shorter synthesis times, the silica walls do not have sufficient time to condense optimally, resulting in a strong shrinkage upon calcination.

Galarneau[19] has shown recently that the unit cell of SBA-15 before calcination is constant and that differences in the unit cell of the calcined material should be attibuted to a different degree of shrinkage. We have found that the unit cell of the uncalcined SBA-16 materials, prepared under the conditions of Table 1, is in all cases 14.0 ± 0.2 nm. However, after calcination of these materials, one can observe in Table 1 a clear increase in the unit cell as a function of increasing stirring time and, to a lesser extent, as a function of increasing aging time. Well condensed samples have a final unit cell after calcination of approximately 13.4 nm. Optimum synthesis times are therefore 8 h or more stirring and 24 h or more aging.

Effect of the TEOS/P127 Ratio. Changing the TEOS/surfactant ratio has important effects on the porosity of the final

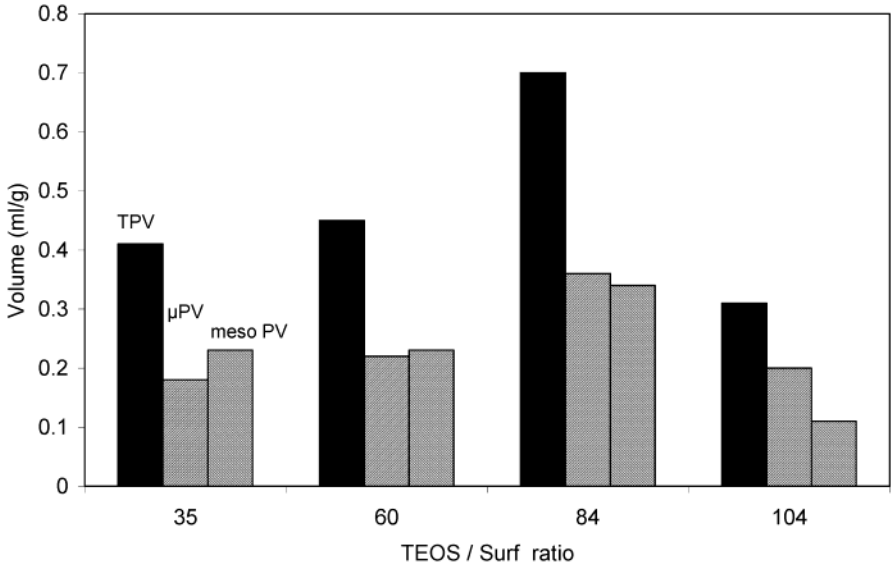

Figure 6. Evolution of the total, micro- and mesopore volume as a function of the TEOS/surfactant ratio. All other synthesis parameters are held constant (see caption of Figure 5).

TABLE 1: Properties of SBA-16 Materials Prepared at Different Stirring and Aging Times. SA_{BET}: BET Surface Area, TPV: Total Pore Volule, μPV: Micropore Volume, D_p: Pore Diameter; a_0: Unit Cell Dimension and h_w: Wall Thickness

	time (hours)	SA_{BET} (m^2/g)	TPV (cc/g)	μ PV (cc/g)	meso PV (cc/g)	D_p (nm)	a_0 (nm)	h_w (nm)
stirring	4	660	0.42	0.19	0.23	4.74	12.1	5.7
time	8	754	0.45	0.22	0.23	5.37	12.4	5.3
	20	939	0.61	0.27	0.34	5.60	13.4	5.9
aging	15	623	0.37	0.17	0.20	4.76	12.4	5.9
time	24	754	0.45	0.22	0.23	5.37	12.4	5.3
	48	815	0.53	0.22	0.31	5.60	12.7	5.4

The values of the other synthesis parameter are described in the capture of Figure 5.

TABLE 2: Properties of SBA-16 Materials Prepared with Different TEOS/Surfactant ratios. SA_{BET}: BET Surface Area, TPV: Total Pore Volume, μPV: Micropore Volume, D_p: Pore Diameter; a_0: Unit Cell Dimension and h_w: Wall Thickness

TEOS/surfactant molar ratio	SA_{BET} (m^2/g)	TPV (cc/g)	μPV (cc/g)	mesopore volume (cc/g)	D_p (nm)	a_0 (nm)	h_w (nm)
35	665	0.41	0.18	0.23	4.8	12.7	6.2
60	754	0.45	0.22	0.23	5.4	12.4	5.3
84	1055	0.70	0.31	0.39	5.6	12.7	5.4
104	622	0.31	0.20	0.11	3.8		

materials. We have changed the TEOS/surfactant ratio from 35 to 104, holding all other parameters constant (stirring temperature 45 °C, stirring time 8 h, aging temperature 80 °C, aging time 24 h).

The results are presented in Figure 6 and Table 2. The total porosity of the SBA-16 sample has a distinct maximum at a TEOS/surfactant ratio of 84. Also, it is important to note that the relative amount of micropores increases continuously as function of increasing TEOS concentration.

Miyazama[20] has discussed the effect of the TEOS/surfactant ratio in the synthesis of SBA-15 and concluded that this a very effective way to increase the microporosity of the samples. He attributed this increase in microporosity mainly to an increase in the (average) wall thickness of the SBA-15 samples and a higher density of the micropores. However, a close inspection of Table 3 shows that we do not observe significant changes in the wall thickness as a function of the TEOS/surfactant ratio. On the contrary, the wall thickness seems to decrease very slightly as a function of increasing TEOS/surfactant ratio. The relative amount (and even absolute amount up to TEOS/surfactant = 84) of micropores increases very strongly as function of the TEOS/surfactant ratio and the unit cell remains virtually constant.

Van Der Voort[21] showed very recently that when the TEOS/surfactant ratio in the synthesis gel of SBA-15 is increased more drastically (doubled or tripled compared to the original ratio of 60), an entirely new material is formed, the so-called PHTS (Plugged Hexagonal Templated Silica). This material consists of the typical hexagonal SBA-15 cylindrical mesopores, with thick and microporously perforated walls. However, on top of that, internal microporous silica plugs exist inside the cylindrical pores, giving rise to a very typical and unique *two step* desorption isotherm. Based on detailed NLDFT calculations and high-resolution TEM, the authors concluded that the high-pressure desorption step can be attributed to the desorption of the open fraction of the pores and the low-pressure desorption step to the fraction of the mesopores that are "blocked" by the plugs. The typical two step isotherm is only observable when the silica plugs are big enough to block the pore in such a way that only a microporous exit is left. This is very comparable to the so-called ink-bottle pores, in which the desorption of the nitrogen is delayed until the magical point of 0.42, after which spinodal decomposition of the nitrogen layer occurs. It is therefore not unreasonable to suggest that Miyazama has observed similar effects, but that in his case, the microporous silica plugs were insufficiently large to completely block the pores. That could also explain the apparent increase in the wall thickness. Moreover, it was apparent from Figure 1 and the theoretical arguments derived from the NLDFT model[17] that the desorption isotherm of a SBA-16 material always closes very near to the point of spontaneous spinodal decomposition of the nitrogen layer, making the analysis of the hysteresis to asses the presence of inkbottle pores or obstructions extremely difficult.

This strongly supports our suggestion that at high TEOS/surfactant ratios, microporous plugs will be formed inside the three-dimensional pore system, hereby strongly increasing the

amount of micropores in the system. The microporosity of the plugs may have following origin. It is known that Pluronic triblock copolymers are in fact polydisperse mixtures of several triblock copolymers with a wide range of molecular weights, and that they contain appreciable amounts of diblock copolymers and even free PO chains. Some of these components, especially the low molecular weight ones, may not be involved in the actual templating of the mesopores, but still act as templates for the disordered nanocapsules, inducing a complementary porosity.

Conclusions

The total pore volume, pore size and relative fraction of micro- and mesopores in the cubic SBA-16 are highly controllable by changing the synthesis temperature, synthesis time and TEOS/surfactant ratio. The contribution of micropores in SBA-16 is unprecedentedly high and can amount up to 65% of the total pore volume. The wall thickness is typically 5−6 nm.

It is suggested that these highly microporous forms of SBA-16, prepared by a very high TEOS/surfactant ratio, contain internal microporous silica nanocapsules, contributing to the added microporosity of these materials. Such materials have also been prepared for the hexagonal SBA-15 counterpart.

The different synthesis parameters, governing the properties of the final material have now been rationalized, allowing a controlled and tailor-made synthesis of the cubic SBA-16 materials.

Acknowledgment. This research was funded by a grant from the University of Antwerp (Special Research Fund) and by the FWO (Flemish Fund for Scientific Research). P.V.D.V. acknowledges the FWO−Flanders for financial support. The authors are grateful to drs. Anna Worobiec for performing the SEM measurements and to Dr. Peter Ravikovitch for NLDFT calculations.

References and Notes

(1) Kresge, C. T.; Leonowicz, M. E.; Roth, W. J.; Vartuli, J. C.; Beck, J. S. *Nature* **1992**, *359*, 710.

(2) Beck, J. S.; Vartuli, J. C.; Roth, W. J.; Leonowicz, M. E.; Kresge, C. T.; Schmitt, T.; Chu, C. T. W.; Olson, D. G.; Sheppard, W.; McCullen, S. B.; Higgins, J. B.; Schlenker, J. L. *J. Am. Chem. Soc.* **1992**, *114*, 10 834.

(3) Inagaki, S.; Fukushima, Y.; Kuroda, K. *Chem. Commun.* **1993**, 680.

(4) Bagshaw, S. A.; Prouzet, E.; Pinnavaia, T. J. *Science* **1995**, *269*, 1242.

(5) Ryoo, R.; Kim, J. M.; Ko, C. H.; Shin, C. H. *J. Phys. Chem.* **1996**, *100*, 17 718.

(6) Zhao, D.; Feng, J.; Huo, Q.; Melosh, N.; Fredrickson, G. H.; Chmelka, B.; Stucky, G. D. *Science* **1998**, *279*, 548.

(7) Zhao, D.; Huo, Q.; Feng, J.; Chmelka, B.; Stucky, G. D. *J. Am. Chem. Soc.* **1998**, *120*, 6024.

(8) Ryoo, R.; Ko, C. H. *J. Phys. Chem. B* **2000**, *104*, 11 465.

(9) Impéror-Clerc, M.; Davidson, A.; Davidson, P. *J. Am. Chem. Soc.* **2000**, *122*, 11 925.

(10) Luan, Z.; Maes, E. M.; Van der Heide, P. A. W.; Zhao, D.; Czernuszewicz, R. S.; Keven, L. *Chem. Mater.* **1999**, *11*, 3680.

(11) Yue, Y.; Gérédon, A.; Bonardet, J. L.; Melosh, N.; D′Espinose, J. B.; Fraissart, J. *Chem. Commun.* **1999**, 1967.

(12) Liu, A. M.; Hidajat, K.; Kawi, S.; Zhao, D. *Chem. Commun.* **2000**, 1145.

(13) Marcowitz, M. A.; Klaehn, J.; Hendel, R. A.; Qadriq, S. L.; Golledge, D. G.; Castner, D. G.; Gaber, B. P. *J. Phys. Chem. B* **2000**, *104*, 10 820.

(14) Yiu, H. H. P.; Botting, C. H.; Botting, N. P.; Wright, P. A. *Phys. Chem. Chem. Phys.* **2001**, *3*, 1145.

(15) Sakamoto, Y.; Kaneda, M.; Terasaki, O.; Zhao, D. Y.; Kim, J. M.; Stucky, G. D.; Shin, H. Y.; Ryoo, R. *Nature* **2000**, *408*, 449.

(16) Schumacher, K.; Ravikovitch, P. I.; Chesne, A. D.; Neimark, A. V.; Unger, K. K. *Langmuir* **2000**, *16*, 4648.

(17) Ravikovitch, P. I.; Neimark, A. V. *Langmuir* **2002**, *18*, 911.

(18) Kruk, M.; Jaroniec, M.; Ko, C. H.; Ryoo, R. *Chem. Mater.* **2000**, *12*, 1961.

(19) Galarneau, A.; Cambon, H.; Di Renzo, F.; Fajula, F. *Langmuir* **2001**, *17*, 8328.

(20) Miyazawa, K.; Inagaki, S. *Chem. Commun.* **2000**, 2121.

(21) Van Der Voort, P.; Ravikovitch, P. I.; De Jong, K. P.; Neimark, A. V.; Janssen, A. H.; Benjelloun, M.; Van Bavel, E.; Cool, P.; Weckhuysen, B. M.; Vansant, E. F. *Chem. Commun.* **2002**, 1010.